

Interfacial Stress Intensity Factors for Edge-Cracked Bonded Semicircles and Strips Under Out-of-Plane Shear

Chih-Hao Chen, Chien-Chung Ke & Chein-Lee Wang

International Journal of Fracture

ISSN 0376-9429

Volume 180

Number 1

Int J Fract (2013) 180:119-127

DOI 10.1007/s10704-012-9797-9



Your article is protected by copyright and all rights are held exclusively by Springer Science +Business Media Dordrecht. This e-offprint is for personal use only and shall not be self-archived in electronic repositories. If you wish to self-archive your work, please use the accepted author's version for posting to your own website or your institution's repository. You may further deposit the accepted author's version on a funder's repository at a funder's request, provided it is not made publicly available until 12 months after publication.

INTERFACIAL STRESS INTENSITY FACTORS FOR EDGE-CRACKED BONDED SEMICIRCLES AND STRIPS UNDER OUT-OF-PLANE SHEAR

Chih-Hao Chen^{1,*}, *Chien-Chung Ke*², *Chein-Lee Wang*³¹*Institute of Applied Mechanics, National Taiwan University, Taipei 106, Taiwan*²*Geotechnical Engineering Research Center, Sinotech Engineering Consultants, Inc., Taipei 110, Taiwan*³*Department of Resources Engineering, National Cheng Kung University, Tainan 701, Taiwan***e-mail: chenhowardch@gmail.com, Corresponding Author*

Abstract. Analytical expressions of the mode III interfacial stress intensity factor are derived for the edge-cracked problems in bonded semicircles and strips. The results are extracted from the solutions of the bonded finite sector by the conformal mapping method. Based on the method, the stress intensity factors for the problems with various crack lengths are achieved, and two corresponding cases are presented and discussed. The obtained solutions can serve as a reference for related crack problems.

Keywords: crack, stress intensity factor, out-of-plane shear, mode III.

1. Introduction. Stress intensity factor (SIF) is one of the important parameters used for analyzing a crack problem. Many studies have been devoted to extracting the SIFs for the crack problems of bonded materials under out-of-plane shear (e.g., Choi et al., 1994; Lee and Earmme, 2000; Li, 2001; Wu and Dzenis, 2002; Shahani, 2003). Finite or semi-infinite cracks lying on the bonded interface were considered in the previous studies. However, the interface used was semi-infinite or infinite. In practice, the length of the bonded interface can be finite, and the crack usually occurs at the edge of the bonded interface. Therefore, the analytical analyses of crack problems with a finite-length bonded interface cannot be neglected. Recently, Chen et al. (2009, 2012) have studied the problems of a crack lying on and terminated at the finite-length bonded interface. Based on the results, this study aims to extract the SIF solutions by the conformal mapping method for two edge-cracked bonded problems in which the crack length is variable with respect to the finite-length interface. Analytical SIF expressions for the two problems for the respective cases are presented and discussed. The obtained results can be used as reference data for related crack problems and serve as a reference for designing the mode III interfacial fracture toughness tests.

2. Interfacial stress intensity factor of a mode III edge crack between two bonded semicircles. Chen et al. (2009) obtained explicit solutions for the bonded finite sectors under out-of-plane shear. In the case with the apex angle of 2π , the problem reduces to that in Fig. 1 (b), and the stress component $\tau_{\theta z}^{(1)}$ of material 1 reduces to

$$\tau_{\theta z}^{(1)} = \frac{2F}{(R+1)\pi} \sum_{n=0}^{\infty} \left\{ \begin{aligned} & \left\{ R \sin \left[\frac{(2n+1)}{2} \beta \right] + \sin \left[\frac{(2n+1)}{2} \alpha \right] \right\} \cos \left[\frac{(2n+1)}{2} \theta \right] \left(\frac{r}{a} \right)^{\frac{2n-1}{2}} \\ & + R \left\{ \cos \left[(n+1) \beta \right] - \cos \left[(n+1) \alpha \right] \right\} \sin \left[(n+1) \theta \right] \left(\frac{r}{a} \right)^n \end{aligned} \right\}, \quad (1)$$

where $R = \mu_1/\mu_2$ and μ_1 and μ_2 denote the shear moduli of the two materials.

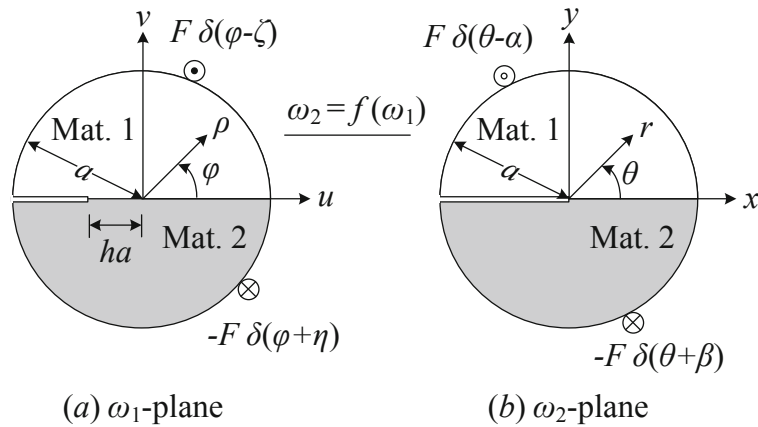


Figure 1. A bonded semicircle containing an edge crack: (a) $a(1-h)$; (b) a in length.

With some manipulation, Eq. (1) may be written as the real part of a complex analytic function in the ω_2 -plane as

$$\tau_{\theta z}^{(1)} = \text{Re} \left\{ \frac{-iFae^{i\theta}}{(R+1)\pi} \left[\left(\frac{a}{\omega_2} \right)^{\frac{1}{2}} \left[\frac{Re^{i\frac{1}{2}\beta}}{a - \omega_2 e^{i\beta}} + \frac{Re^{i\frac{1}{2}(\beta-2\theta)}}{a - \omega_2 e^{i(\beta-2\theta)}} + \frac{e^{i\frac{1}{2}\alpha}}{a - \omega_2 e^{i\alpha}} + \frac{e^{i\frac{1}{2}(\alpha-2\theta)}}{a - \omega_2 e^{i(\alpha-2\theta)}} \right] + R \left[\frac{e^{i\beta}}{a - \omega_2 e^{i\beta}} + \frac{e^{-i\beta}}{a - \omega_2 e^{-i\beta}} + \frac{e^{i\alpha}}{a - \omega_2 e^{i\alpha}} + \frac{e^{-i\alpha}}{a - \omega_2 e^{-i\alpha}} \right] \right] \right\}. \quad (2)$$

$$= \text{Re}[\Lambda'(\omega_2)]$$

Notice that $\omega_2 = re^{i\theta}$.

As shown in Fig. 1, the conformal mapping

$$\omega_2 = f(\omega_1) = \frac{a(\omega_1 + ha)}{a + \omega_1 h}, \quad (3)$$

where $-1 < h < 1$, will map the region in Fig. 1(a) onto the region in Fig. 1(b).

The complex function $\Lambda'(\omega_2)$ can be expressed in terms of the complex variable ω_1 in the ω_1 -plane as

$$\Lambda'(\omega_1) = \frac{-iFae^{i\varphi}}{\pi(R+1)} \left\{ \left(\frac{a}{\omega_2} \right)^{\frac{1}{2}} \left[\frac{Re^{i\frac{1}{2}\beta}}{a-\omega_2e^{i\beta}} + \frac{Re^{i\frac{1}{2}(\beta-2\varphi)}}{a-\omega_2e^{i(\beta-2\varphi)}} + \frac{e^{i\frac{1}{2}\alpha}}{a-\omega_2e^{i\alpha}} + \frac{e^{i\frac{1}{2}(\alpha-2\varphi)}}{a-\omega_2e^{i(\alpha-2\varphi)}} \right] + R \left[\frac{e^{i\beta}}{a-\omega_2e^{i\beta}} + \frac{e^{-i\beta}}{a-\omega_2e^{-i\beta}} + \frac{e^{i\alpha}}{a-\omega_2e^{i\alpha}} + \frac{e^{-i\alpha}}{a-\omega_2e^{-i\alpha}} \right] \right\} \times \omega_2'(\omega_1)$$

(4)

It is noted that the relation Eq. (3) should be applied to Eq. (4), along with the following relationships:

$$e^{i\alpha} = \frac{h + e^{i\zeta}}{1 + he^{i\zeta}}, \quad e^{i\beta} = \frac{h + e^{i\eta}}{1 + he^{i\eta}},$$

(5)

where ζ and η are the respective loading angles applied to materials 1 and 2 in the problem of Fig. 1(a).

Thus, the interfacial SIF in the problem of Fig. 1(a) can be derived using the definition (Hellan, 1984):

$$K_{III} = \lim_{\substack{\omega_1 \rightarrow -ah \\ \varphi \rightarrow 0}} \sqrt{2\pi(\omega_1 + ah)} \Lambda'(\omega_1),$$

(6)

and this results in

$$K_{III} = s_1 \sqrt{\sqrt{a_1^2 + b_1^2} - a_1} + s_2 \sqrt{\sqrt{a_2^2 + b_2^2} - a_2},$$

(7)

where

$$s_1 = \frac{2F}{R+1} \sqrt{\frac{a}{\pi(1-h^2)[1+h^2+2h\cos(\zeta)]}}, \quad s_2 = \frac{2FR}{R+1} \sqrt{\frac{a}{\pi(1-h^2)[1+h^2+2h\cos(\eta)]}},$$

$$a_1 = 2h + (h^2 + 1)\cos(\zeta), \quad b_1 = (1-h^2)\sin(\zeta),$$

$$a_2 = 2h + (h^2 + 1)\cos(\eta), \quad b_2 = (1-h^2)\sin(\eta).$$

(8)

For the case with $h = 0$, the SIF reduces to

$$K_{III} = \frac{2F}{R+1} \sqrt{\frac{2a}{\pi}} \left[\sin\left(\frac{\zeta}{2}\right) + R \sin\left(\frac{\eta}{2}\right) \right],$$

(9)

which is identical to the result obtained by Chen et al. (2009).

For the case with $\zeta = \eta$ (i.e., the same loading angles), the SIF reduces to

$$K_{III} = (s_1 + s_2) \sqrt{\sqrt{a_1^2 + b_1^2} - a_1},$$

(10)

which becomes independent of the ratio of the material properties, R .

3. Interfacial stress intensity factor of a mode III edge crack between two bonded strips.

In a similar manner to that used in the previous section, the conformal mapping

$$\omega_2 = f(\omega_3) = a \tan \left[\frac{\pi(\omega_3 + ha)}{4(a + \omega_3 h)} \right],$$

(11)

where $-1 < h < 1$, will map the region in Fig. 2(a) onto the region in Fig. 2(b).

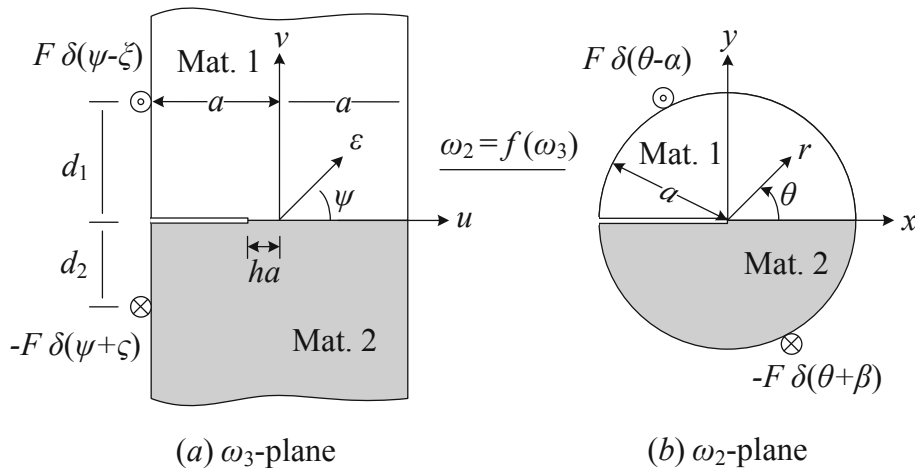


Figure 2. (a) A bonded strip containing an edge crack $a(1-h)$ in length; (b) A bonded semicircle containing an edge crack a in length.

The complex function $\Lambda'(\omega_2)$ can be expressed in terms of the complex variable ω_3 in the ω_3 -plane as

$$\Lambda'(\omega_3) = \frac{-iFae^{i\psi}}{\pi(R+1)} \left\{ \left(\frac{a}{\omega_2} \right)^{\frac{1}{2}} \left[\frac{Re^{\frac{i}{2}\beta}}{a - \omega_2 e^{i\beta}} + \frac{Re^{\frac{i}{2}(\beta-2\psi)}}{a - \omega_2 e^{i(\beta-2\psi)}} + \frac{e^{\frac{i}{2}\alpha}}{a - \omega_2 e^{i\alpha}} + \frac{e^{\frac{i}{2}(\alpha-2\psi)}}{a - \omega_2 e^{i(\alpha-2\psi)}} \right] + R \left[\frac{e^{i\beta}}{a - \omega_2 e^{i\beta}} + \frac{e^{-i\beta}}{a - \omega_2 e^{-i\beta}} + \frac{e^{i\alpha}}{a - \omega_2 e^{i\alpha}} + \frac{e^{-i\alpha}}{a - \omega_2 e^{-i\alpha}} \right] \right\} \times \omega'_2(\omega_3)$$

(12)

Equation (11) should be applied to Eq. (12), along with the following relationships:

$$e^{i\alpha} = \tan \left[\frac{\pi(\rho_1 e^{i\xi} + ha)}{4(a + \rho_1 h e^{i\xi})} \right], \quad e^{i\beta} = \tan \left[\frac{\pi(\rho_2 e^{i\zeta} + ha)}{4(a + \rho_2 h e^{i\zeta})} \right],$$

(13)

where ξ and ζ are the respective loading angles applied to materials 1 and 2 in the problem of Fig. 2(a), $\rho_1 = \sqrt{a^2 + d_1^2}$, $\rho_2 = \sqrt{a^2 + d_2^2}$, and d_1 and d_2 are vertical distances from the respective loading points to the interface.

Thus, the interfacial SIF in the problem of Fig. 2(a) can be derived as

$$K_{III} = S_1 \sqrt{\sqrt{A_1^2 + B_1^2} - A_1} + S_2 \sqrt{\sqrt{A_2^2 + B_2^2} - A_2}, \tag{14}$$

where

$$S_1 = \frac{F\sqrt{a}}{(R+1)\sqrt{1-h^2}}, \quad S_2 = \frac{FR\sqrt{a}}{(R+1)\sqrt{1-h^2}}, \tag{15}$$

and $A_1, B_1, A_2,$ and B_2 have to be determined according to (I) $\xi < \pi/2$ and $\zeta < \pi/2$, (II) $\xi > \pi/2$ and $\zeta < \pi/2$, (III) $\xi < \pi/2$ and $\zeta > \pi/2$, and (IV) $\xi > \pi/2$ and $\zeta > \pi/2$, respectively. In case of (IV) $\xi > \pi/2$ and $\zeta > \pi/2$, for example, gives

$$A_i = \frac{\sin \left\{ \frac{\pi \left[-a^2(1-h)^2 + h d_i^2 \right]}{2 \left[a^2(1-h)^2 + h^2 d_i^2 \right]} \right\}}{\cos \left\{ \frac{\pi \left[-a^2(1-h)^2 + h d_i^2 \right]}{2 \left[a^2(1-h)^2 + h^2 d_i^2 \right]} \right\} + \cosh \left\{ \frac{\pi a d_i (1-h^2)}{2 \left[a^2(1-h)^2 + h^2 d_i^2 \right]} \right\}},$$

$$B_i = \frac{\sinh \left\{ \frac{\pi a d_i (1-h^2)}{2 \left[a^2 (1-h)^2 + h^2 d_i^2 \right]} \right\}}{\cos \left\{ \frac{\pi \left[-a^2 (1-h)^2 + h d_i^2 \right]}{2 \left[a^2 (1-h)^2 + h^2 d_i^2 \right]} \right\}} + \cosh \left\{ \frac{\pi a d_i (1-h^2)}{2 \left[a^2 (1-h)^2 + h^2 d_i^2 \right]} \right\}}, \quad (16)$$

where $i=1, 2$.

For the case with $h = 0$, the SIF reduces to

$$K_{III} = \frac{F\sqrt{a}}{R+1} \left(\sqrt{1 + \operatorname{sech} \left(\frac{\pi d_1}{2a} \right)} + R \sqrt{1 + \operatorname{sech} \left(\frac{\pi d_2}{2a} \right)} \right), \text{ if } \xi > \pi/2 \text{ and } \zeta > \pi/2. \quad (17)$$

For the case with $\xi = \zeta$ (the same loading angles), the SIF reduces to

$$K_{III} = \frac{F\sqrt{a}}{\sqrt{1-h^2}} \sqrt{\sqrt{A_1^2 + B_1^2} - A_1}, \quad (18)$$

where A_1 and B_1 refer to Eq. (16). Similarly, the SIF is independent of the ratio of the material properties.

For the case with $R=1$ (the single material case), the SIF reduces to

$$K_{III} = \frac{F\sqrt{a}}{2\sqrt{1-h^2}} \left(\sqrt{\sqrt{A_1^2 + B_1^2} - A_1} + \sqrt{\sqrt{A_2^2 + B_2^2} - A_2} \right), \quad (19)$$

where $A_1, B_1, A_2,$ and B_2 refer to Eq. (16).

4. Case study. As shown in Fig. 3, two cases will be discussed in this section based on the solutions obtained above. Cases 1 and 2 are the interfacial edge-cracked problems of two bonded semicircles and two bonded strips. The SIF solutions for the respective cases are obtained from Eqs. (7) and (14) with the given conditions.

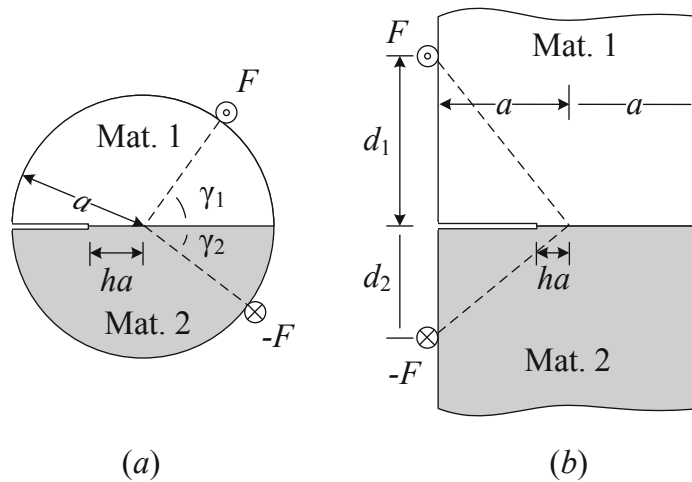


Figure 3. The case study: (a) Case 1 (bonded semicircles); (b) Case 2 (bonded strips).

4.1 Case 1 – the interfacial edge-cracked problem of two bonded semicircles. For $h=\pm 0.5$, and $R=0.5$ and 1.5 , the dimensionless SIF ($F_{III}=K_{III}/Fa^{1/2}$) distributions, with $0\leq\gamma_1\leq\pi$ and $0\leq\gamma_2\leq\pi$, are listed in Table 1. The table shows that at $h=0.5$, γ_1 is more sensitive than γ_2 to the SIF with $R=0.5$, while the opposite is true for the SIF with $R=1.5$. At $h=-0.5$, the small loading angles are sensitive to the SIF. These results indicate that the loads on the softer material dominates the SIF for the case with a shorter crack length ($h=0.5$) and the loads close to the crack tip dominates the SIF for the case with a longer crack length ($h=-0.5$). In addition, the maximum and minimum SIFs occur at the loading angles of both π and 0 . Given $\gamma_1=\pi/2$ and $\gamma_2=3\pi/4$, the dimensionless SIF versus h is plotted in Fig. 4(a), showing that a decrease in h (an increase in the crack length) results in an increase in the SIF. Little SIF difference between the results of the three material combinations is obtained if the crack length is reduced close to zero or the crack cuts through most of the interface. Moreover, increasing R increases the SIF because γ_2 is greater than γ_1 .

4.2 Case 2 – the interfacial edge-cracked problem of two bonded strips. For $h=\pm 0.5$ and $R=0.5$ and 1.5 , the dimensionless SIF ($F_{III}=K_{III}/Fa^{1/2}$) distributions, with $0\leq x_1(d_1/a)\leq 1$ and $0\leq x_2(d_2/a)\leq 1$, are listed in Table 2. The table shows that within the applied loading distance, a decrease in x_1 (or x_2) results in an increase in the SIF while $h=0.5$ but a decrease in the SIF while $h=-0.5$. In addition, only a slight SIF variation is obtained for this case. Given $x_1=1/2$ and $x_2=3/4$, the dimensionless SIF versus h is plotted in Fig. 4(b), showing that the results are close, especially for those of $h<0$. The results from $h=1$ to -1 show that the SIF first increases rapidly and then drops a little, and finally, it increases with the decrease in h (an increasing crack length). This indicates that there is a stable crack growth stage for this case if an edge crack initiates and extends along the interface.

Table 1. The dimensionless SIF distributions for Case 1.

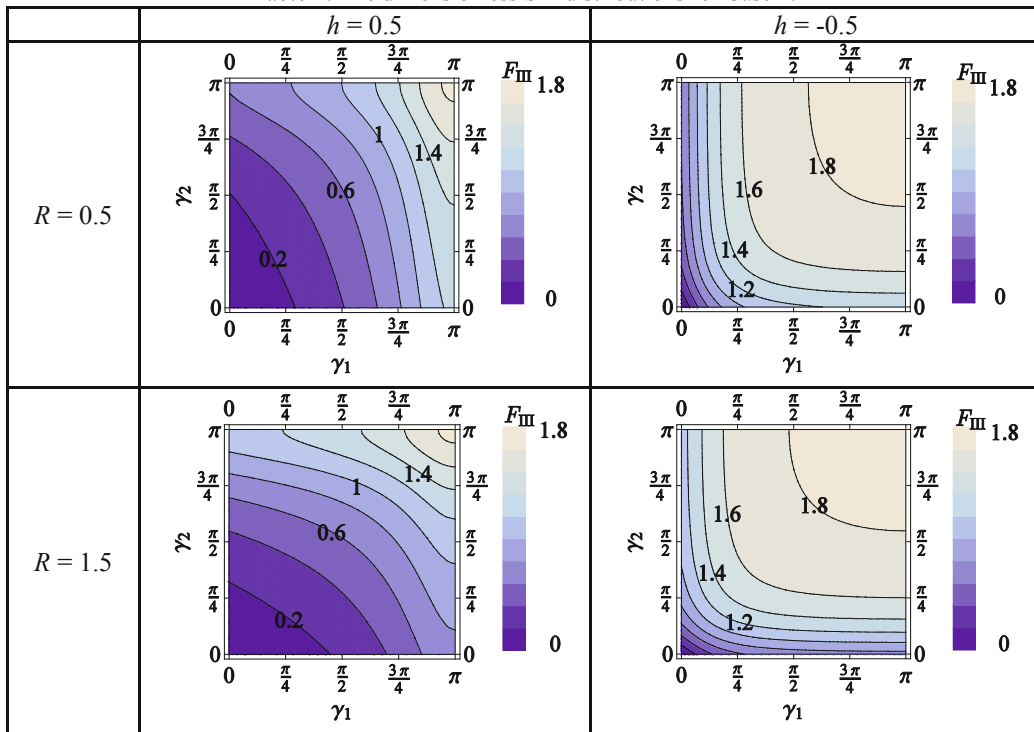
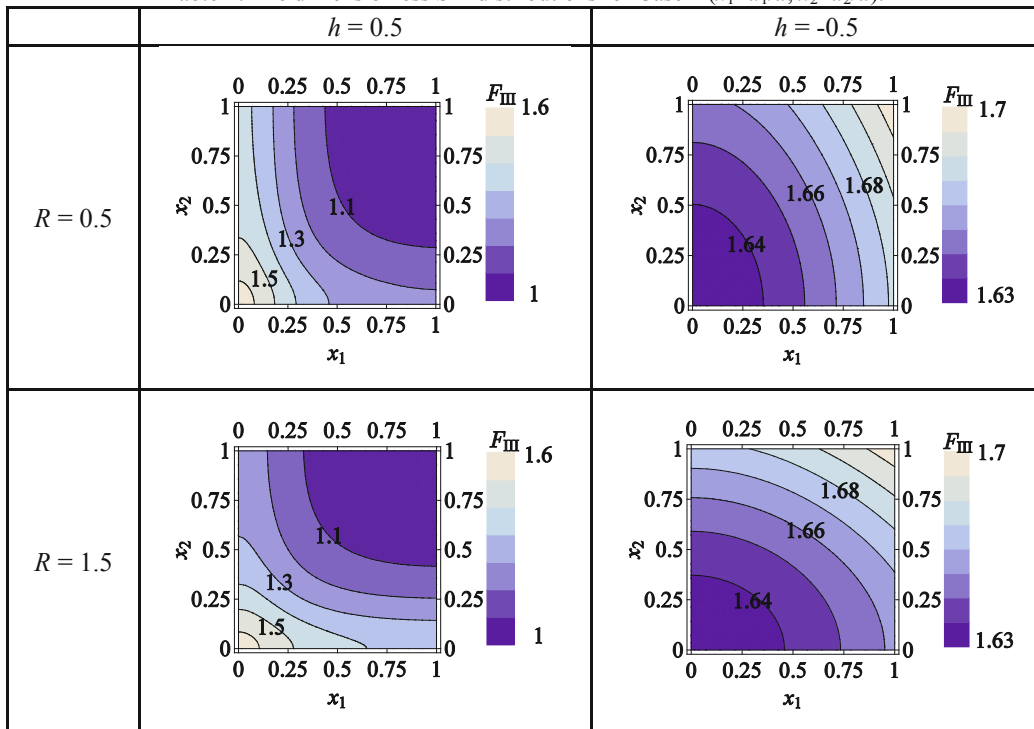


Table 2. The dimensionless SIF distributions for Case 2 ($x_1=d_1/a, x_2=d_2/a$).



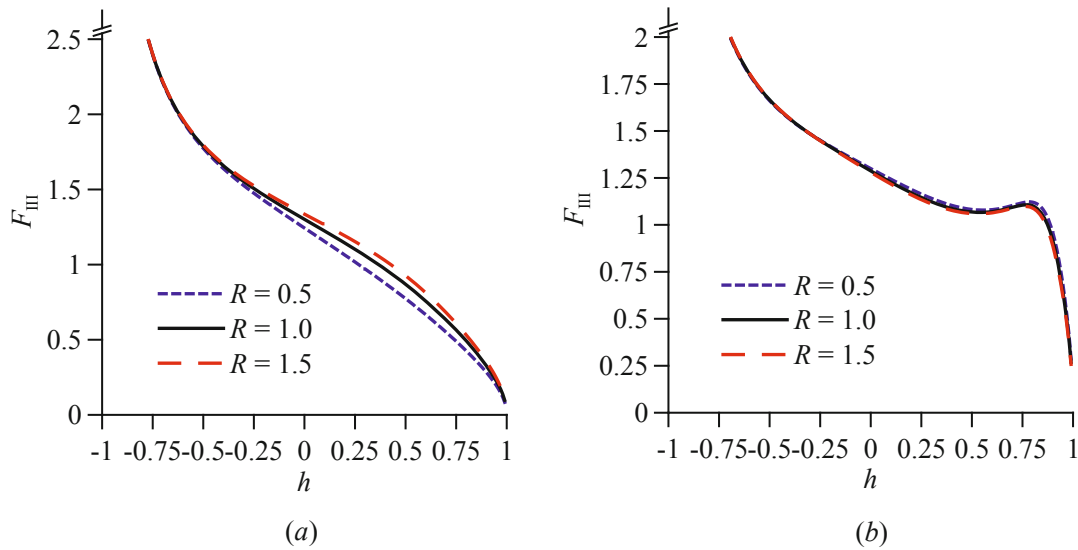


Figure 4. The dimensionless SIF versus h : (a) Case 1 with $\gamma_1 = \pi/2$ and $\gamma_2 = 3\pi/4$; (b) Case 2 with $x_1 = 1/2$ and $x_2 = 3/4$.

5. Conclusions. Two interfacial edge-cracked problems under out-of-plane shear are analyzed. Stress intensity factors for these problems are derived from the solutions obtained in Chen et al. (2009) by the conformal mapping method. Using the derived solutions, the SIF distributions for the respective cases are presented and discussed. The derived SIF solutions can be applied to the problems with various crack lengths and material ratios, and those can be used as the reference data for the related crack problems.

References

- Chen, C.H., Wang, C.L., Ke, C.C. (2009). Analysis of composite finite wedge under anti-plane shear. *Int J Mech Sci* **51**, 583-597.
- Chen, C.H., Wang, C.L., Kuo, C.C. (2012). Solutions for anti-plane problems of a composite material with a crack terminating at the interface. *Arch Appl Mech* **82**, 1233-1250.
- Choi, S.R., Chong, C.H., Chai, Y.S. (1994). Interfacial edge crack in two bonded dissimilar orthotropic quarter planes under anti-plane shear. *Int J Fract* **67**, 143-150.
- Hellan, K. (1984). Introduction to fracture mechanics. McGraw-Hill, New York.
- Lee, K.W., Earmme, Y.Y. (2000). An interfacial edge crack in anisotropic bimaterial under anti-plane singularity. *Int J Fract* **104**, 15-22.
- Li, X.F. (2001). Closed-form solution for a mode-III interface crack between two bonded dissimilar elastic layers. *Int J Fract* **109**, L3-L8.
- Shahani, A.R. (2003). Mode III stress intensity factors for edge-cracked circular shafts, bonded wedges, bonded half planes and DCB's. *Int J Solids Struct* **40**, 6567-6576.
- Wu, X.F., Dzenis, Y.A. (2002). Closed-form solution for a mode-III interfacial edge crack between two bonded dissimilar elastic strips. *Mech Res Commun* **29**, 407-412.